Nucleosomal Stability and Dynamics Vary Significantly When Viewed by Internal Versus Terminal Labels[†]

Laimonas Kelbauskas,*[,‡] Jenny Sun,[‡] Neal Woodbury,[‡,§] and D. Lohr[§]

Biodesign Institute, and Department of Chemistry and Biochemistry, Arizona State University, Tempe, Arizona 85287

Received January 15, 2008; Revised Manuscript Received June 29, 2008

ABSTRACT: Nucleosomes are a major impediment to regulatory factor activities and therefore to the operation of genomic processes in eukaryotes. One suggested mechanism for overcoming *in vivo* nucleosomal repression is factor-mediated removal of H2A/H2B from nucleosomes. Using nucleosomes labeled internally with FRET fluorophores, we previously observed significant, DNA sequence-dependent variation in stability and dynamics under conditions (subnanomolar concentrations) reported to produce H2A/H2B release from nucleosomes. Here, the same analytical approaches are repeated using 5S and MMTV-B nucleosomes containing FRET labels that monitor the terminal regions. The results show that stability and dynamics vary significantly within the nucleosome; terminally labeled constructs report significantly reduced stability and enhanced DNA dynamics compared to internally labeled constructs. The data also strongly support previous suggestions (1) that subnanomolar concentrations cause H2A/H2B release from nucleosomes, including the 5S, and (2) that stabilities in the internal regions of 5S and two promoter-derived nucleosomes (MMTV-B, *GAL10*) differ. Sequence-dependent nucleosome stability/dynamics differences could produce inherent variations in the accessibility of histone-associated DNA *in vivo*. Such intrinsic variation could also provide a mechanism for producing enhanced effects on specific nucleosomes by processes affecting large chromatin regions, thus facilitating the localized targeting of alterations to nucleosomes on crucial regulatory sequences. The results demonstrate clearly the importance of studying physiologically relevant nucleosomes.

Nucleosomes are the basic units of eukaryotic chromosome structure. They consist of a histone octamer, one H3/H4 tetramer, and two H2A/H2B dimers, wrapped by slightly less than two superturns (~147 bp) of DNA (*1, 2*). The tetramer contacts mainly the central DNA region, ~60 bp around the nucleosome dyad; H2A/H2B dimers bind to adjacent, ~30 bp DNA regions located toward the termini (Figure 1; (*2*)). The high genomic levels of nucleosome coverage (cf. *3, 4*), including their presence on regulatory DNA sequences such as promoters (*5–9*), and the pronounced tendency of nucleosomes to restrict regulatory factor access to DNA have combined to generate intense interest in mechanisms that can produce nucleosomal DNA exposure, because of their potential impact on the operation of *in vivo* processes.

The nucleosome is dynamic and its structure can change as a result of intrinsic or factor-mediated processes (*10*). For example, nucleosomal DNA exists transiently in a reversible, partially histone-dissociated state (*11–13*), providing an intrinsic mechanism for DNA exposure. The histones also exhibit dynamic behavior. H2A/H2B undergo rapid exchange in and out of nucleosomes *in vivo* (*14*) and H2A/H2B release

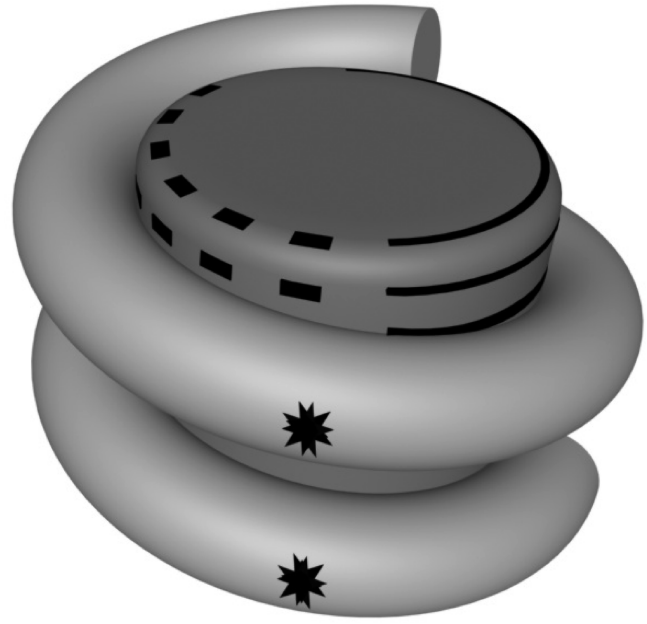

FIGURE 1: FRET-labeled nucleosomes. To apply FRET approaches (cf. ref *48*.) to nucleosomes, ~150−160 bp DNA fragments (Materials and Methods) were labeled with FRET donor (Cy3) and acceptor (Cy5) fluorophores at internal sites ~80 bp apart (*30*). Reconstitution of this DNA into nucleosomes brings the fluorophores close, due to the 80 bp/gyre nucleosomal wrap, producing efficient energy transfer between the fluorophores (stars) and a strong FRET signal. The regions of H2A/H2B histone-DNA (dashed line) and H3/H4 histone-DNA contact (solid line) in the top half of the nucleosome (based on ref *2*) are identified schematically.

[†] This work was supported by National Science Foundation Grants PHY-0239986 (to N.W. and D.L.), PHY-0631631 (to N.W.), NIH Grant Ca 85990 (to D.L.), and Science Foundation of Arizona Grant CAA 0122-07 (to N.W.).

* To whom correspondence should be addressed. Biodesign Institute, Arizona State University, Tempe, AZ 85287-6501. Phone: (480) 965 3128. Fax: 480 727 6588. E-mail: laimonas.kelbauskas@asu.edu.

[‡] Biodesign Institute.

[§] Department of Chemistry and Biochemistry.

10.1021/bi8000775 CCC: $40.75
Published on Web 08/15/2008

is produced by the action of transcription-associated complexes *in vitro*, including RNA polymerase (*15*), transcription elongation complexes (*16*), ATP-dependent nucleosome remodeling complexes (*17, 18*) and the histone chaperone yNAP-1 (*19*). H2A/H2B loss could provide a way to enhance DNA accessibility, at least in the regions where H2A/H2B bind (Figure 1), while still maintaining a histone presence via the H3/H4 tetramer.

Variability in the inherent properties of individual nucleosomes in a chromatin fiber could play a role in the *in vivo* regulation of genomic processes (*20*). Nucleosomes with unique intrinsic DNA dynamics could create sites with inherently enhanced (or diminished) factor accessibility. Nucleosomes with unique stability properties could create sites with inherently enhanced (or diminished) ability to undergo the kinds of transitions occurring during factor-mediated, nucleosome alteration processes.

DNA sequence-associated differences are an obvious potential source of nucleosome variation *in vivo* and sequence-dependent features have been observed *in vitro* using various biochemical approaches (*21*). Recently, using Förster resonance energy transfer (FRET[1]) techniques, we have detected some significant, DNA sequence-dependent stability and dynamics variations in nucleosomes (*13, 21*). FRET is a powerful and sensitive approach for the study of conformational features in biological macromolecules. FRET occurs when an excited donor fluorophore lies close (typically 1−5 nm) to an appropriate acceptor fluorophore. A sixth power dependence on fluorophore separation makes FRET extremely sensitive to the kinds of distance changes (donor to acceptor) that occur during conformational transitions, whether spontaneous or factor-induced. FRET-based approaches can be applied at single molecule or bulk levels and have been used in several nucleosome studies (*11, 22–29*).

Our FRET approach involves labeling a DNA fragment (~160 bp) with donor (Cy3) and acceptor (Cy5) fluorophores at sites 80 bp apart within the DNA fragment (*30*). When such labeled DNA is reconstituted into a nucleosome, donor and acceptor fluorophores are brought into close proximity by the nucleosomal wrap (Figure 1), allowing efficient energy transfer and producing a strong FRET signal. Nucleosome conformational changes can be detected as FRET changes, usually decreases. Note that free (non-nucleosomal) DNA gives no FRET signal in our system (*30*).

We have used this approach to compare nucleosomes reconstituted on three natural DNA sequences (*21*): a TATA-containing sequence from the yeast *GAL10* promoter (*31*); a sequence containing four of the six glucocorticoid receptor (GR) binding elements from the MMTV promoter (*32*); and 5S rDNA, a widely used standard (*33*). The two pol II promoter fragments were chosen for study because *in vivo* those sequences reside in nucleosomes that undergo significant and functionally important structural changes during transcription activation (*31, 32*). All three sequences reconstitute into typical nucleosomes and for each, a single, dominant position is observed on gels (*13, 21*), in accord with the known ability of each sequence to position nucleosomes (5S (*34, 35*), MMTV-B (*36, 37*), and *GAL10* (*31*)).

[1] Abbreviations: FRET, Förster resonance energy transfer; PCR, polymerase chain reaction; MMTV-B, mouse mammary tumor virus nucleosome B; FCS, fluorescence correlation spectroscopy; pol II, RNA polymerase II.

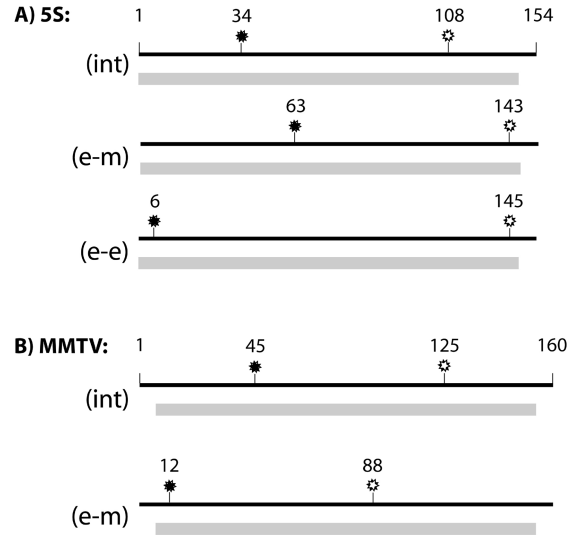

FIGURE 2: Fluorophore placements. Fluorophore positions (stars) are located to scale on the DNA fragments (black lines), with numbers given in bp from the left end of the fragment, and on the major nucleosome positions (gray bars) for 5S (panel a) and MMTV-B (panel b). Internally labeled nucleosomes (int): DNA fragments are labeled so that the fluorophores lie within the nucleosome, ~30−40 bp from each terminus. Note that fluorophores cannot always be placed exactly 80 bp apart because of sequence restrictions. End−middle labeled nucleosomes (e-m): DNA fragments are labeled so that one fluorophore lies near the nucleosome terminus and the other close to the nucleosome center, again as close to 80 bp apart as possible. End−end labeled 5S nucleosomes (e-e): DNA fragments are labeled so that fluorophores lie close to each nucleosome terminus. Nucleosomes with terminal DNA labels have been widely used in FRET studies (*11, 22–26, 28, 29*), but the combination of an internal and a terminal DNA label (e-m) is less common (*49*).

We have found that 5S and the pol II promoter nucleosomes differ in a number of structural (diffusion coefficients/intrinsic FRET efficiencies), stability (with respect to salt, temperature, and concentration), and dynamics (reversible DNA−histone association) features (*13, 21*). Differences may be even greater than those we observe because the fluorophores are located at the maximum FRET-yielding positions in the MMTV-B and *GAL10* nucleosomes but not in the 5S (for technical reasons). All the differences indicate that 5S nucleosomal complexes are more stable and less dynamic than MMTV-B or *GAL10* complexes, including greater stability under conditions reported to cause H2A/H2B release from nucleosomes. Given the association of H2A/H2B release with transcription factor activity (above) and the roles of *GAL10* and MMTV-B nucleosome structural changes in the *in vivo* transcription activation process on their associated genes (*31, 32*), these differences (versus the 5S) could have functional significance.

In our previous work, DNA fragments were labeled so that the fluorophores would bracket the center and thus lie well within the reconstituted nucleosome, ~30−40 bp from each terminus ((*21*); Figure 2). However, the location of H2A/H2B-DNA binding sites in the nucleosome (Figure 1) suggests that H2A/H2B loss might have greater effects on the terminal than on the internal regions. Thus, here, we have placed the FRET fluorophores in locations that can directly monitor responses of the terminal nucleosomal regions.

The results show that terminally labeled complexes, 5S or MMTV-B, exhibit a number of features indicating that

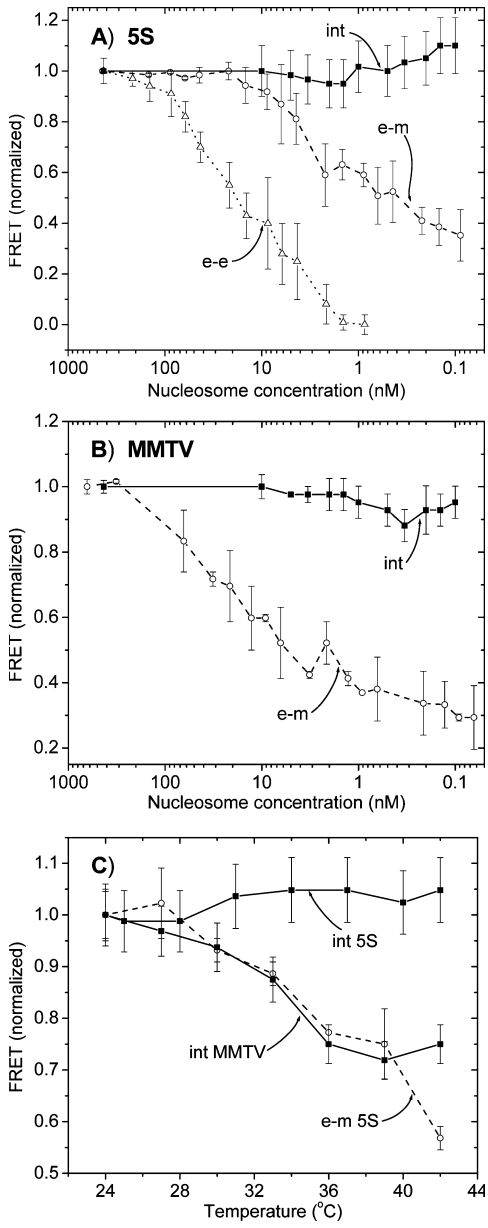

FIGURE 3: Terminally-labeled 5S nucleosomes are quite sensitive to dilution or heating. FRET efficiency (energy transfer, see Materials and Methods) is plotted as a function of nucleosome concentration (panels A and B) or temperature (panel C) for internally labeled 5S or MMTV-B (■, solid lines), end−middle labeled 5S or MMTV-B (○, dashed lines), or end−end labeled 5S (△, dotted lines) samples. Values are normalized to initial conditions, high concentration/22 °C (panels A and B) and 22 °C/0.2 nM nucleosome concentrations (panel C). The temperature studies are carried out at subnanomolar concentrations, to provide more information on nucleosomal particles under these (depletion) conditions. Raw, unnormalized data is shown in Supporting Information, Figures S2a−c.

the terminal regions have reduced stability and elevated DNA dynamics compared to the internal regions. Thus, dynamics and stability can vary significantly within the nucleosome, at least between the regions monitored here (see Figures 2 and S1 (Supporting Information). Results with the 5S constructs provide strong support for our suggestion that H2A/H2B loss produces different effects in 5S compared to the promoter-derived nucleosomes due to differential strengths of DNA−histone binding in the internal regions of the complexes. This set of results has potentially important consequences for mechanisms of nucleosomal DNA access.

MATERIALS AND METHODS

DNA and Nucleosome Preparation. Fluorescently labeled dsDNA fragments (∼160 bp in length) were made by PCR techniques, using the appropriate DNA templates and fluorescently labeled primers (*30*). The DNA fragments used in this work have been described in detail (*21*): a 154 bp sea urchin 5S rDNA fragment corresponding to the region between the 5′ *Eco*RI and Ban II sites (*34*); an MMTV fragment (−70 to −230 bp on the promoter) that corresponds to the *in vivo* position of nucleosome B (*36*).

In previous work, DNA fragments were labeled so that the fluorophores would be internal, ∼30−40 bp from each nucleosome terminus (*21*). Fluorophore locations in the nucleosome can be varied by changing the fluorophore positions in the primers used to make the labeled DNA fragments. In this work, two types of terminally labeled nucleosomes were made. End−middle labeled (e-m) nucleosomes contain fluorophores located 63 bp and 4 bp from the nucleosome termini (63 bp and 11 bp from the DNA fragment termini) for 5S (Figure 2a) and 5 bp and 64 bp from the nucleosome termini (12 bp and 72 bp from the DNA fragment termini) for MMTV-B (Figure 2b). End−end labeled 5S nucleosomes (Figure 2a e-e) contain fluorophores located 6 bp and 2 bp from the nucleosome termini (6 bp and 9 bp from the DNA fragment termini). In the internally labeled nucleosomes (int, Figure 2a, 2b), fluorophores lie 34 bp and 39 bp from the nucleosome termini (34 bp and 46 bp from the DNA fragment termini) for 5S and 38 bp and 27 bp from the nucleosome termini (45 and 35 bp from the DNA fragment termini) for MMTV-B. Note that fluorophores cannot always be placed exactly 80 bp apart because of labeling restrictions. After PCR, the labeled DNA is gel-purified, then reconstituted into nucleosomes by salt-step dialysis using HeLa histone octamers, as described previously (*38*). The histone octamers were a generous gift from Dr. J. Yodh. The histone/DNA ratios that gave mostly mononucleosomes, with little free DNA or higher bands on polyacrylamide gels, were empirically determined.

Fluorescence Techniques. Concentration dependence, temperature dependence, single molecule distributions and fluorescence correlation spectroscopy (FCS) were all carried out as described previously (*13, 21*) in 10 mM Tris/1 mM EDTA buffer at pH 8. Nucleosome concentrations were determined by comparing the relative fluorescence intensities of free DNA samples at known concentrations and nucleosome samples of unknown concentration using the following formalism:

$$I_{\mathrm{DNA}} = gC_{\mathrm{DNA}}, I_{\mathrm{nucl}} = gC_{\mathrm{nucl}} \Rightarrow \frac{I_{\mathrm{DNA}}}{C_{\mathrm{DNA}}} = \frac{I_{\mathrm{nucl}}}{C_{\mathrm{nucl}}} \Rightarrow C_{\mathrm{nucl}} = \frac{I_{\mathrm{nucl}} C_{\mathrm{DNA}}}{I_{\mathrm{DNA}}} \quad (1)$$

where I_{DNA} and I_{nucl} are the total fluorescence intensities obtained from the free DNA sample (known concentration) and the nucleosome sample of interest (unknown concentration), respectively, C_{DNA} and C_{nucl} are the concentrations of the free DNA and the nucleosome samples, respectively, and

g represents a factor that accounts for the excitation intensity, fluorescence quantum yield of the markers, and emission collection/detection efficiency The fluorescence quantum yields of naked DNA and nucleosome samples did not show significant differences.

FRET efficiency was calculated using the following equation:

$$E_{\mathrm{FRET}} = \frac{I_{\mathrm{A}}}{I_{\mathrm{A}} + \gamma I_{\mathrm{D}}} \tag{2}$$

where I_A and I_D are the fluorescence intensities measured in the acceptor and donor channel, respectively, and $\gamma = 1.12$ is a factor correcting for the cross-talk between the detection channels, differences in detection efficiency, or in fluorescence quantum yield, and any contribution from direct excitation of the acceptor. E_{FRET} errors were calculated as the standard error of mean (S.E.M.) using $\Delta E_{FRET} = \sigma/N^{1/2}$, where σ is the standard deviation and N is the number of independent measurements.

As noted previously (*21*), the effects of temperature on the emission properties of fluorophores were found to be comparable for both the Cy3 and Cy5 dyes. Because the calculation of the FRET efficiency is based on the ratios of donor and acceptor emission intensity and not on their absolute values, the emission intensity changes caused by temperature increase should cancel each other. We found that the relative change in FRET efficiency resulting from the temperature effect is <2% at 40 °C and <1% at 30 °C. Also, the key observations in our analyses involve differences between nucleosome types and fluorophore locations in the constructs; such differences should not be due to dye photophysical effects since all three types were made and studied in the same way. For the FRET distributions, the binning time was 1 ms. We have shown that under these conditions of analysis, the system shows two-state behavior (*13*). It is possible that under other analysis conditions, such as faster time scales, nucleosome transition behavior would show greater complexity. However, this should not significantly affect the data analysis shown here in terms of a two state model.

Fluorescence Correlation Spectroscopy (FCS). We previously used FCS techniques to study nucleosome dynamics (*13*). The transitions that our probes monitor in these particles occur between a high-FRET, closed state (C) and a low-FRET open state (O) and show two-state behavior. Thus,

$$\mathrm{C} \underset{k_{21}}{\overset{k_{12}}{\rightleftharpoons}} \mathrm{O} \tag{3}$$

where k_{12} and k_{21} are the rate constants for forward and backward conformational changes, respectively, in the complexes. FCS detects fluctuations in FRET signals, which can arise from particle diffusion and/or conformational transitions. We found that in solution, diffusion dominated the FCS signal; therefore, measurements were performed on particles embedded in agarose gels to decrease the diffusion rates. To separate the two contributions to the FCS signal, molecules with a single label (Cy3-labeled, diffusion only) and double-labeled molecules (Cy3/Cy5, conformational transitions that change the FRET plus diffusion) were analyzed (separately). This allows the use of standard techniques to analyze the FCS signal (see eq S1, Supporting Information). The analysis yields values for the average time a particle spends in the open and the closed states. Ref *13* and http://www.public.asu.edu/~lkelbaus/ can be consulted for more detail about this analysis. Note that our goal in this work is to obtain relative values of these parameters for the three types of particles not absolute values.

RESULTS

Terminally-Labeled Nucleosomes. Internally labeled 5S and MMTV-B (or *GAL10*) nucleosomes differ in their response to subnanomolar concentrations or treatment with the histone chaperone yNAP-1 (*13, 21*). Since both conditions cause H2A/H2B release from the nucleosome (*39, 19*), these differences were attributed to differing effects produced by the loss of H2A/H2B. To monitor the regions that should be the most strongly affected by H2A/H2B loss and thus test this conclusion, terminally labeled nucleosome constructs were made by placing fluorophores either (1) near the terminus and the nucleosome center, ~80 bp apart (e-m, Figure 2a and b), or (2) near each terminus (e-e, Figure 2a). Both types of terminally labeled nucleosomes show gel mobilities that are very similar to those of the corresponding internally labeled nucleosomes and thus form similar nucleosome structures. However, average FRET values are lower (data not shown), which would be expected given the suggested lability of DNA around nucleosome termini (*40–42*).

Many of our studies are carried out at subnanomolar concentrations, that is, concentrations even lower than those shown to cause H2A/H2B release (*39*). Complexes at subnanomolar concentrations (H2A/H2B-depleted nucleosomes) will be referred to as particles to distinguish them from intact nucleosomes. Subnanomolar concentrations are required in some cases (cf. Figure 4) or give more consistent results (cf. Table 1). These conditions also stress the H3/H4−H2A/H2B association−dissociation equilibrium, thus allowing a comparison of the response of the three different types of nucleosomes to that stress.

Dilution Studies of Nucleosomes. Terminally labeled (end−middle, e-m; Figure 2a) 5S nucleosomes show significant FRET decreases with increasing dilution (Figure 3a, open circles). The normalized FRET efficiency (defined in Materials and Methods (eq 2)) begins to drop sharply at ~10 nM and decreases consistently with further dilution. In contrast, internally labeled 5S nucleosomes (Figure 3a, filled squares) show no FRET decreases down to 100 pM concentration. This is ~40-fold lower than the concentrations that produce major H2A/H2B loss in 601 nucleosomes (*39*).

The data in Figure 3a demonstrates clearly that 5S nucleosomes do undergo a substantial change in response to dilution to nanomolar and subnanomolar concentrations, but it is necessary to monitor the terminal regions to detect the change. Note that terminally and internally labeled nucleosomes are identical except for the positions of the fluorophores. Studies with 601 nucleosomes reported major H2A/H2B loss by ~5 nM (*39*), the same concentration range in which terminally labeled 5S nucleosomes (Figure 3a) and internally labeled MMTV-B and *GAL10* nucleosomes (*13*) show strong FRET decreases. This similarity indicates that H2A/H2B loss is probably responsible for the FRET decreases in all three complexes. H2A/H2B ease of dissocia-

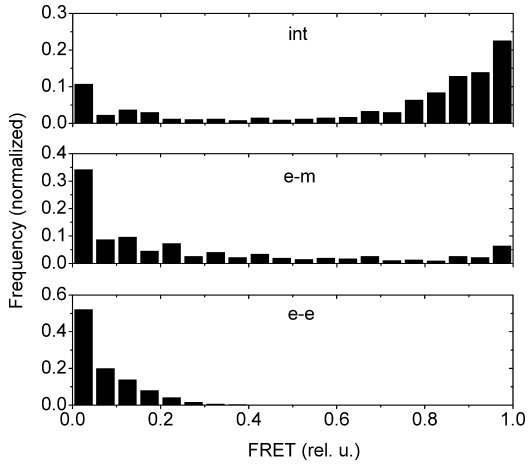

FIGURE 4: Single molecule FRET efficiency population distributions. The FRET efficiencies of individual nucleosome complexes were determined in solution at 0.2 nM concentration. Distributions of FRET efficiency for internally labeled (int), end−middle labeled (e-m), or end−end labeled (e-e) 5S particles are shown, with FRET efficiency plotted on the *x*-axis and the normalized frequency (normalized to the total number of individual molecules observed in the experiment) plotted on the *y*-axis. Note that only molecules with DNA wrapped around histones, e.g., H2A/H2B-depleted particles, can give FRET; free DNA gives no FRET signal (*30*). Molecules with low or no FRET can reflect unreconstituted DNA (present in similar amounts in all samples), particles from which the DNA has dissociated or particles that were transiently unfolded as they went through the excitation beam (*13*). The presence of (the few) intermediate FRET molecules in the distribution may reflect particles undergoing transitions while in the beam, less than infinite cooperativity in the system, etc.

tion should depend mainly on the strength of the H2A/H2B−H3/H4 interaction and thus should be similar among nucleosomes since this interaction is probably well-conserved (*1, 2*). The response differences in Figure 3a thus indicate that H2A/H2B is lost at subnanomolar concentrations (Figure 3a, e-m) but this loss has little effect on the internal regions of 5S complexes Figure 3a, int).

End−end labeled 5S nucleosomes (e-e, Figure 2a) show even larger FRET decreases upon dilution (Figure 3a, open triangles). The significant lability of terminal DNA (*40, 42*) plus greater inherent fluorophore separation due to particle geometry (see Figure 1) probably account for the greatly enhanced sensitivities noted with end−end labeled nucleosomes. Equilibrium constants are also much lower for end−end than for end−middle labeled 5S nucleosomes (data not shown). Low FRET and extreme sensitivity make end−end labeled constructs much less suitable for study than end−middle labeled constructs. End−middle labeled constructs also have other advantages. Fluorophores are 80 bp apart, as in internally labeled constructs; and the behavior of a single terminus is monitored.

Terminally labeled (end−middle, e-m; Figure 2b) MMTV-B nucleosomes are also more sensitive to dilution than internally labeled constructs (Figure 3b, filled squares vs open circles) and more dilution-sensitive than terminally labeled 5S nucleosomes (Figure 3a vs b). The latter indicates lower stability for MMTV-B versus 5S nucleosomes; a similar conclusion was made for internally labeled 5S and MMTV-B nucleosomes (*21*).

Complete DNA dissociation from the histone octamer has also been reported at subnanomolar concentrations, using gel analyses (cf. (*43*)). This process could contribute to the FRET decreases observed during dilution in our solution studies (Figure 3a and b). However, if complete DNA dissociation were the only process being monitored in our studies, then altering the location of the FRET labels in nucleosomes that are otherwise identical should not strongly affect the results; complete dissociation of DNA would give the same FRET loss no matter where the fluorophores were located. However, label location clearly matters (Figure 3a and b). Thus, dilution must induce a change that strongly and specifically affects the terminal regions, such as H2A/H2B loss. Moreover, studies carried out at the end-point concentration of the dilution studies, 0.2 nM, show clear evidence for the presence of (large numbers of) DNA−histone complexes (see below). Note also that the solution conditions used in ref *43* differ from those used here.

Heating Studies of Particles. Heating to ∼40 °C frees ∼20 bp of DNA around each nucleosome terminus (*40*). Heating produces major FRET decreases, starting well below 40 °C, in terminally labeled (end−middle) but not in internally labeled 5S particles (Figure 3c, open circles vs filled squares). This difference directly demonstrates that in 5S particles, DNA−histone binding in the internal regions is strong enough to keep internal fluorophores close together, even when the terminal regions are highly mobile, as they would be at elevated temperatures. In contrast, heating of internally labeled MMTV-B (Figure 3c) or *GAL10* (*21*) particles causes significant FRET decreases. Thus, DNA−histone binding in the internal regions of these particles is not strong enough to keep internal fluorophores close together. Terminally labeled MMTV-B particles are more sensitive to heating than internally labeled MMTV-B particles (data not shown).

Single Molecule Distributions. Single molecule optical techniques (see Materials and Methods) applied at low enough particle concentrations (>1 nM) allow FRET signals to be detected one molecule at a time. By counting large numbers of individual molecules, one can obtain a single molecule population distribution, the relative numbers of molecules vs FRET efficiency, for a given sample. This plot shows the precise distribution of molecular conformations in the sample, as monitored by the FRET fluorophores in the constructs.

Such distributions show significant numbers of high FRET efficiency (0.8−1.0) molecules, for all three types of internally labeled complexes (cf. Figure 4, int (*13*)). High FRET efficiency indicates a canonically wrapped and dynamically stable structure, at least with respect to DNA (and fluorophores) in the internal regions of the particle.

However, distributions for samples of terminally labeled 5S complexes show no (end−end) or very low (end−middle) numbers of high FRET efficiency molecules (Figure 4, e-e, e-m). Again these constructs are identical except for the fluorophore positions. This data illustrates the enhanced strength of the DNA−histone interaction in the internal versus the terminal regions of 5S particles. MMTV-B samples also show a major loss of high FRET efficiency molecules in distributions from terminally (end−middle) versus internally labeled complexes (Supporting Information, Figure S3).

DNA Dynamics in Particles. Fluorescence Correlation Spectroscopy (FCS) techniques were used previously (*13*) to compare the dynamics in internally labeled 5S, MMTV-B and *GAL10* particles (subnanomolar concentrations). The

Table 1: Equilibrium and DNA Dynamics Data For Nucleosomes and Nucleosomal Particles[a]

complex type	K_{part}[b] (rel. u.)	k_{conf}[c] (s^{-1})	τ_{open}[d] (ms)	τ_{closed}[e] (ms)	K_{nucl}[f] (rel. u.)
5S (int)[g]	1.20 ± 0.14	54 ± 8	34 ± 7	41 ± 8	1.20 ± 0.12
5S (e-m) [g]	0.10 ± 0.01	9 ± 4	99 ± 40[h]	10 ± 4	0.96 ± 0.10
MMTV (int)	0.69 ± 0.08	42 ± 14	58 ± 19	40 ± 13	1.00 ± 0.10
MMTV (e-m)	0.2 ± 0.03	18 ± 6	108 ± 37[h]	22 ± 7	1.15 ± 0.20[i]
GAL10 (int)	0.44 ± 0.05	40 ± 10	82 ± 22	36 ± 10	0.73 ± 0.07

[a] All values are given as mean ± SE. Note that we have also carried out the FCS experiments at higher concentrations, conditions under which nucleosomes remain intact, but the results have been highly variable, even for internally labeled nucleosomes. Why this should be the case remains unclear. One possible explanation could be that at higher concentrations nucleosomal dynamics become more complex and thus cannot be approximated by a two-state model, as required for the calculations. [b] Equilibrium constants (association) for DNA−histone complexes at subnanomolar concentrations, i.e., particles. [c] Calculated by fitting eq S1 (Supporting Information) to the experimental data. [d,e] Open and closed residence times, calculated using eq S2 (Supporting Information) and $\tau_{closed} = 1/k_{12}$, $\tau_{open} = 1/k_{21}$. [f] Equilibrium constants (association) for intact nucleosomes (bulk concentration ~150 nM). [g] int, internally labeled complexes; e-m, end−middle labeled complexes. End−end labeled complexes show insufficient FRET for analysis at these concentrations. [h] The high uncertainties are due to the low levels of FRET in terminally labeled complexes. [i] The significance, if any, of the differences in closed times for terminally labeled 5S vs MMTV nucleosomes complexes is unclear. The terminal label is closer to the end in the 5S construct (Figure 2), and this may account for this behavior. Note that we have also carried out the FCS experiments at higher concentrations, conditions under which nucleosomes remain intact, but the results have been highly variable, even for internally labeled nucleosomes. Why this should be the case remains unclear. One possible explanation could be that at higher concentrations nucleosomal dynamics become more complex and thus cannot be approximated by a two-state model, as required for the calculations.

dynamic process monitored by these DNA-linked fluorophores involves reversible, transient fluorophore separation and probably reflects a DNA−histone association−dissociation process. This process exhibits two-state behavior (*13*). Transitions occur between a high FRET efficiency (≥0.8), closed state in which the DNA is canonically and stably wrapped on the particle, keeping the fluorophores close enough together, on average, for strong energy transfer, and a low FRET efficiency (<0.2), open state in which the fluorophores are too far apart, on average, for significant energy transfer to occur. There is no significant population of molecules in intermediate conformational states.

FCS studies can provide biologically useful information about such transitions, such as the average residence times in the open (τ_{open}) and the closed (τ_{closed}) states. In the open state, DNA should be partially unbound from histones and thus more available for factor binding. In the closed state, DNA should be less available or even unavailable for factor binding. Average residence times in the closed state are similar for the three types of internally labeled particles, but residence times in the open state vary significantly, with 5S having the shortest and *GAL10* the longest open residence time (Table 1).

The dynamics monitored in terminally labeled constructs differ (Table 1). Closed residence times are shorter, and open residence times are much longer than in internally labeled particles, both 5S and MMTV-B. Such changes in inherent DNA dynamics are consistent with the enhanced FRET decreases during dilution or heating (Figure 3) and the reduction in high FRET efficiency molecules in population distributions (Figure 4) of terminally labeled 5S or MMTV-B particles. Shorter closed and longer open residence times are also consistent with a loss of H2A/H2B-DNA contacts (see Figure 1) arising from H2A/H2B release at subnanomolar concentrations.

Equilibrium Constants. Equilibrium constant values were determined for intact nucleosomes (bulk concentrations) and particles (subnanomolar concentrations), for both internally labeled and terminally labeled constructs (Table 1). These values refer again to the reversible DNA−histone association−dissociation process monitored by our FRET probes. The data support the results described above. Most notably, for both 5S and MMTV-B complexes, K_{eq} values differ only slightly between terminally and internally labeled intact nucleosomes, but there are very large differences in K_{eq} values between terminally and internally labeled particles (Table 1). This indicates clearly that a stabilizing feature of the terminal regions is removed by dilution of nucleosomes to subnanomolar concentrations. H2A/H2B is known to stabilize the nucleosome, and H2A/H2B interacts with DNA regions that lie toward the termini (see Figure 1). Thus, K_{eq} data provide very strong support for the conclusion that H2A/H2B is lost from the nucleosome at subnanomolar concentrations. Moreover, the similar (low) K_{eq} values for terminally labeled 5S or MMTV-B particles suggest similar levels of H2A/H2B loss in the two.

These data provide additional insights. The K_{eq} variations for internally labeled particles, 5S > MMTV-B > *GAL10* (Table 1), correlate with open residence time differences (5S < MMTV-B > *GAL10*), that is, the larger the equilibrium constant, the shorter the open residence time. That correlation could indicate that H3/H4 tetramer−DNA affinity (tetramers would be the major histones in H2A/H2B-depleted complexes) is a determinant of open residence times. Equilibrium constant values for intact nucleosomes show the same variation, 5S > MMTV-B > *GAL10*, which is consistent with the significant role of the tetramer in stabilizing nucleosomes (*40*). K_{eq} values for internally labeled 5S nucleosomes or particles are the same (Table 1), indicating that H2A/H2B-depleted 5S nucleosomes are very stable and maintain strong DNA−histone binding. However, K_{eq} values for internally labeled MMTV-B or *GAL10* particles are lower than those for the corresponding intact nucleosomes, indicating a lower stability (and weaker internal region DNA−histone binding) for those particles compared to the nucleosome.

DISCUSSION

In the work presented here, FRET-based approaches were used to study nucleosomes labeled with fluorophores (Cy3/Cy5) in locations that monitor the terminal nucleosomal regions (Figures 2 and S1, Supporting Information). These studies were undertaken for several reasons. First, previous studies comparing internally labeled 5S and two promoter-derived nucleosomes (MMTV-B or *GAL10*) suggested variations associated with H2A/H2B loss. The association of H2A/H2B loss with transcription factor activity (see Introduction)

and the occurrence of crucial, transcription activation-associated structural changes in these MMTV-B and *GAL10* nucleosomes *in vivo* make such differences (versus the 5S) of possible functional significance. H2A/H2B loss should strongly affect the terminal regions so that terminally labeled constructs will directly assess those differences. Second, comparing internally and terminally labeled constructs will provide information on stability and dynamics variations within nucleosome complexes. Third, results obtained with terminally labeled constructs can more readily be compared to work from other laboratories, which have used mainly terminally labeled nucleosomes.

We find that terminally labeled nucleosome complexes, both 5S and MMTV-B, yield quite different results than the same complexes with internal labels. Terminally labeled nucleosomes show a greater sensitivity to dilution (Figure 3a and b), and terminally labeled particles (subnanomolar concentrations) show enhanced sensitivity to heating (Figure 3c), greatly reduced numbers of high FRET molecules (Figure 4), much smaller equilibrium constants, and significantly enhanced DNA dynamics, that is, longer open residence times (Table 1). The fluorophores in these constructs should mainly monitor the behavior of the specific areas in which they are located. Thus, the results show that conformational features in the terminal and internal regions of nucleosomal complexes can vary significantly. Although the responses of 5S and MMTV-B complexes are qualitatively similar, effects are typically greater in MMTV-B complexes. Thus, these intranucleosomal variations can show DNA sequence dependence, that is, variations in degree in different nucleosomes.

Results obtained with the terminally labeled 5S constructs strongly support previous suggestions that FRET differences at subnanomolar concentrations between internally labeled 5S and MMTV-B or *GAL10* complexes arise from differing effects produced by H2A/H2B loss (*13, 21*). These results include confirmation that 5S nucleosomes do undergo change in response to dilution (Figure 3a, e-m) and equilibrium constant changes at subnanomolar concentrations that strongly indicate H2A/H2B loss (see Results). The observation that yNAP-induced H2A/H2B release produces the same response differences as dilution (*13*) also supports this conclusion. The differing responses to H2A/H2B loss are suggested to reflect differences in internal region DNA−histone binding strength (*13*); strong binding in 5S particles keeps the fluorophores close and prevents energy transfer changes, but weaker binding in MMTV-B and *GAL10* particles is unable to do so. Other observations support this suggestion: (1) K_{eq} values for (internally labeled) 5S nucleosomes and particles are similar, but K_{eq} values for MMTV-B or *GAL10* particles are lower than those for nucleosomes (*13*); (2) terminal DNA release (by heating) causes FRET decreases in terminally or internally labeled MMTV-B and *GAL10* particles and in terminally labeled but not in internally labeled 5S particles (Figure 4); (3) 5S DNA binds strongly to octamers (cf. (*44*)) or to H3/H4 tetramers (*45*); (4) DNA−histone interactions are strongest in the central ~100 bp regions of nucleosomes containing other strong histone-binding DNA sequences (*2, 46*).

Complete DNA−octamer dissociation can also occur at subnanomolar concentrations (cf. (*43*)) and would cause FRET decreases in our dilution studies (Figure 3a and b). However, the striking effects produced by changing probe locations within the nucleosome (Figures 3a and b, and 4; Table 1) are only consistent with an effect involving and specifically destabilizing the terminal regions of the nucleosome, such as H2A/H2B loss (also see Results). Also, in our system, FRET only occurs in canonically wrapped DNA−histone complexes, nucleosomes, or particles (*30*); therefore, FCS data (Table 1) or high FRET particles (Figure 4) clearly indicate the presence of such complexes.

Subnanomolar concentrations are of course not physiological but must be used for some techniques, for example, single molecule analysis. However, these conditions also provide the opportunity to compare the relative stabilities of these different types of nucleosomes under conditions that stress the association/dissociation equilibrium. The information obtained, cf. 5S vs MMTV-B, should be valid under any conditions. Therefore, the conclusions that nucleosomes can exhibit sequence-dependent variations in stability/dynamics and differ in effects produced by H2A/H2B loss should apply to physiological conditions as well as to subnanomolar concentrations. *In vivo*, factors could exploit these kinds of differences to produce specific, localized effects (see below).

The occurrence of DNA sequence-dependent stability and dynamics variations between nucleosomes (*13, 21*) raises the important possibility that inherent nucleosome properties could affect the accessibility of nucleosomal DNA to regulatory factors *in vivo*. This has significant consequences for mechanisms of nucleosome exposure and the regulation of genomic processes. Variation in stability and dynamics within nucleosomes, as observed here, has important consequences as well. Such intranucleosomal variability implies that simple descriptions of nucleosome properties may not be meaningful since properties vary depending on where in the nucleosome they are monitored. For example, the extremely low stability and enhanced dynamics of the constructs with both labels in terminal regions (end−end labeled) indicates that those commonly used types of constructs may provide an exaggerated view of nucleosome lability and one that is not characteristic of the more internal regions of the nucleosome. The apparent sequence dependence infers that intranucleosomal variability may not be the same in all nucleosome complexes. For example, H2A/H2B depletion has little effect on internal region stability in 5S complexes but significant effects on the stability of these regions in MMTV-B and *GAL10* complexes. Intranucleosomal variability in stability and dynamics also suggests that the precise location of a DNA regulatory element within the nucleosome is important and even relatively small changes in its location, for example, from the nucleosome center to the terminus, could have major consequences for its intrinsic accessibility and the ability of the region in which it resides to undergo conformational change.

Sequence-dependent variations in intrinsic stability and dynamics, whether intra- or internucleosomal, could impact nucleosome targeting. Enhanced DNA dynamics (longer open residence times), cf. MMTV-B/*GAL10* vs 5S particles or terminal vs internal regions (Table 1), could significantly enhance the intrinsic accessibility of nucleosomal DNA sequences. Low stability could allow nucleosomes or particles to undergo structural transitions that are associated with functional processes more easily and might even act as a *de*

facto targeting mechanism, enabling nonselective, regional chromatin alteration, such as H2A/H2B release or histone acetylation (*47*), to produce enhanced (sequence-specific) effects in particular nucleosomes. Any of these features could facilitate specific nucleosome recognition and thus aid in the crucial targeting process. This model would predict that stability and/or dynamics should vary, in a function-associated manner, for the nucleosomes on a promoter. Indeed, we have obtained evidence for such behavior on the MMTV promoter (Kelbauskas et al., manuscript in preparation). Thus, DNA sequence-dependent nucleosome stability and dynamics variations could have a significant impact on genomic regulation processes. These results also emphasize the importance of studying nucleosomes containing physiologically relevant DNA sequences.

SUPPORTING INFORMATION AVAILABLE

Description of the FCS approach used for the data analysis; locations of the fluorescent labels in the nucleosome (Figure S1); raw, un-normalized versions of the data presented in Figure 3 (Figure S2); single molecule FRET distributions of internally (middle−middle, int) and terminally labeled (end−middle, e-m) MMTV-B particles at 200 pM concentration (Figure S3). This material is available free of charge via the Internet at http://pubs.acs.org.

REFERENCES

1. Van Holde, K., Zlatanova, J., Arents, G., Moudrianakis, E. (1995) In *Chromatin Structure and Gene Expression* (Elgin, S. C., Ed.) 1st ed., pp 1−21, Oxford University Press, Oxford, U.K.
2. Luger, K., Mader, A. W., Richmond, R. K., Sargent, D. F., and Richmond, T. J. (1997) Crystal structure of the nucleosome core particle at 2.8 Å resolution. *Nature 18*, 251–260.
3. Lohr, D., Kovacic, R. T., and Van Holde, K. E. (1977) Quantitative analysis of the digestion of yeast chromatin by staphylococcal nuclease. *Biochemistry 16*, 463–471.
4. Bernstein, B. E., Liu, C. L., Humphrey, E. L., Perlstein, E. O., and Schreiber, S. L. (2004) Global nucleosome occupancy in yeast. *Genome Biol. 5*, R62.
5. Wallrath, L. L., Lu, Q., Granok, H., and Elgin, S. C. (1994) Architectural variations of inducible eukaryotic promoters: preset and remodeling chromatin structures. *BioEssays 16*, 165–170.
6. Hager, G., C. Smith, T. Svaren, W. Hortz (1995) *Initiation of Expression: Remodeling Genes*, Oxford University Press, Oxford, U.K.
7. Lohr, D. (1997) Nucleosome transactions on the promoters of the yeast GAL and PHO genes. *J. Biol. Chem. 272*, 26795–26798.
8. Huebert, D. J., and Bernstein, B. E. (2005) Genomic views of chromatin. *Curr. Opin. Genet. Dev. 15*, 476–481.
9. Barrera, L. O., and Ren, B. (2006) The transcriptional regulatory code of eukaryotic cells insights from genome-wide analysis of chromatin organization and transcription factor binding. *Curr. Opin. Cell Biol. 18*, 291–298.
10. Luger, K., and Hansen, J. C. (2005) Nucleosome and chromatin fiber dynamics. *Curr. Opin. Struct. Biol. 15*, 188–196.
11. Li, G., Levitus, M., Bustamante, C., and Widom, J. (2005) Rapid spontaneous accessibility of nucleosomal DNA. *Nat. Struct. Mol. Biol. 12*, 46–53.
12. Li, G., and Widom, J. (2004) Nucleosomes facilitate their own invasion. *Nat. Struct. Mol. Biol. 11*, 763–769.
13. Kelbauskas, L., Chan, N., Bash, R., DeBartolo, P., Sun, J., Woodbury, N., and Lohr, D. (2008) Sequence-dependent variations associated with H2A/H2B depletion of nucleosomes. *Biophys. J. 94*, 147–158.
14. Kimura, H., and Cook, P. R. (2001) Kinetics of core histones in living human cells: little exchange of H3 and H4 and some rapid exchange of H2B. *J. Cell Biol. 153*, 1341–1353.
15. Studitsky, V. M., Walter, W., Kireeva, M., Kashlev, M., and Felsenfeld, G. (2004) Chromatin remodeling by RNA polymerases. *Trends Biochem. Sci. 29*, 127–135.
16. Reinberg, D., and Sims, R. J. (2006) de FACTo nucleosome dynamics. *J. Biol. Chem. 281*, 23297–23301.
17. Bruno, M., Flaus, A., Stockdale, C., Rencurel, C., Ferreira, H., and Owen-Hughes, T. (2003) Histone H2A/H2B dimer exchange by ATP-dependent chromatin remodeling activities. *Mol. Cell 12*, 1599–1606.
18. Bash, R., Wang, H., Anderson, C., Yodh, J., Hager, G., Lindsay, S. M., and Lohr, D. (2006) AFM imaging of protein movements: Histone H2A-H2B release during nucleosome remodeling. *FEBS Lett. 580*, 4757–4761.
19. Park, Y. J., Chodaparambil, J. V., Bao, Y. H., McBryant, S. J., and Luger, K. (2005) Nucleosome assembly protein 1 exchanges histone H2A-H2B dimers and assists nucleosome sliding. *J. Biol. Chem. 280*, 1817–1825.
20. Giresi, P. G., Gupta, M., and Lieb, J. D. (2006) Regulation of nucleosome stability as a mediator of chromatin function. *Curr. Opin. Genet. Dev. 16*, 171–176.
21. Kelbauskas, L., Chan, N., Bash, R., Yodh, J., Woodbury, N., and Lohr, D. (2007) Sequence-dependent nucleosome structure and stability variations detected by Förster resonance energy transfer. *Biochemistry 46*, 2239–2248.
22. Park, Y. J., Dyer, P. N., Tremethick, D. J., and Luger, K. (2004) A new fluorescence resonance energy transfer approach demonstrates that the histone variant H2AZ stabilizes the histone octamer within the nucleosome. *J. Biol. Chem. 279*, 24274–24282.
23. Bao, Y., Konesky, K., Park, Y. J., Rosu, S., Dyer, P. N., Rangasamy, D., Tremethick, D. J., Laybourn, P. J., and Luger, K. (2004) Nucleosomes containing the histone variant H2A.Bbd organize only 118 base pairs of DNA. *EMBO J. 23*, 3314–3324.
24. Toth, K., Brun, N., and Langowski, J. (2001) Trajectory of nucleosomal linker DNA studied by fluorescence resonance energy transfer. *Biochemistry 40*, 6921–6928.
25. Toth, K., Brun, N., and Langowski, J. (2006) Chromatin compaction at the mononucleosome level. *Biochemistry 45*, 1591–1598.
26. White, C. L., and Luger, K. (2004) Defined structural changes occur in a nucleosome upon Amt1 transcription factor binding. *J. Mol. Biol. 342*, 1391–1402.
27. Tomschik, M., Zheng, H., van Holde, K., Zlatanova, J., and Leuba, S. H. (2005) Fast, long-range, reversible conformational fluctuations in nucleosomes revealed by single-pair fluorescence resonance energy transfer. *Proc. Natl. Acad. Sci. U.S.A. 102*, 3278–3283.
28. Bussiek, M., Toth, K., Schwarz, N., and Langowski, J. (2006) Trinucleosome compaction studied by fluorescence energy transfer and scanning force microscopy. *Biochemistry 45*, 10838–10846.
29. Bao, Y. H., White, C. L., and Luger, K. (2006) Nucleosome core particles containing a poly(dA center dot dT) sequence element exhibit a locally distorted DNA structure. *J. Mol. Biol. 361*, 617–624.
30. Lovullo, D., Daniel, D., Yodh, J., Lohr, D., and Woodbury, N. W. (2005) A fluorescence resonance energy transfer-based probe to monitor nucleosome structure. *Anal. Biochem. 341*, 165–172.
31. Bash, R., and Lohr, D. (2001) Yeast chromatin structure and regulation of GAL gene expression. *Prog. Nucleic Acid Res. Mol. Biol. 65*, 197–259.
32. Hager, G. L. (2001) Understanding nuclear receptor function: from DNA to chromatin to the interphase nucleus. *Prog. Nucleic Acid Res. Mol. Biol. 66*, 279–305.
33. Hansen, J. C. (2002) Conformational dynamics of the chromatin fiber in solution: determinants, mechanisms, and functions. *Annu. Rev. Biophys. Biomol. Struct. 31*, 361–392.
34. Dong, F., Hansen, J. C., and Vanholde, K. E. (1990) DNA and protein determinants of nucleosome positioning on sea-urchin 5S ribosomal-RNA gene-sequences in vitro. *Proc. Natl. Acad. Sci. U.S.A. 87*, 5724–5728.
35. Meersseman, G., Pennings, S., and Bradbury, E. M. (1991) Chromatosome positioning on assembled long chromatin. Linker histones affect nucleosome placement on 5 S rDNA. *J. Mol. Biol. 220*, 89–100.
36. Fragoso, G., John, S., Roberts, M. S., and Hager, G. L. (1995) Nucleosome positioning on the MMTV LTR results from the frequency-biased occupancy of multiple frames. *Genes Dev. 9*, 1933–1947.
37. Fragoso, G., Pennie, W. D., John, S., and Hager, G. L. (1998) The position and length of the steroid-dependent hypersensitive region in the mouse mammary tumor virus long terminal repeat are invariant despite multiple nucleosome B frames. *Mol. Cell. Biol. 18*, 3633–3644.
38. Bash, R. C., Yodh, J., Lyubchenko, Y., Woodbury, N., and Lohr, D. (2001) Population analysis of subsaturated 172−12 nucleosomal

arrays by atomic force microscopy detects nonrandom behavior that is favored by histone acetylation and short repeat length. *J. Biol. Chem. 276*, 48362–48370.
39. Claudet, C., Angelov, D., Bouvet, P., Dimitrov, S., and Bednar, J. (2005) Histone octamer instability under single molecule experiment conditions. *J. Biol. Chem. 280*, 19958–19965.
40. Van Holde, K. (1989) *Chromatin*, Springer Verlag, New York.
41. Polach, K. J., and Widom, J. (1995) Mechanism of protein access to specific DNA-sequences in chromatin - a dynamic equilibrium-model for gene-regulation. *J. Mol. Biol. 254*, 130–149.
42. Anderson, J. D., and Widom, J. (2000) Sequence and position-dependence of the equilibrium accessibility of nucleosomal DNA target sites. *J. Mol. Biol. 296*, 979–987.
43. Thastrom, A., Gottesfeld, J. M., Luger, K., and Widom, J. (2004) Histone - DNA binding free energy cannot be measured in dilution-driven dissociation experiments. *Biochemistry 43*, 736–741.
44. Thastrom, A., Lowary, P. T., Widlund, H. R., Cao, H., Kubista, M., and Widom, J. (1999) Sequence motifs and free energies of selected natural and non-natural nucleosome positioning DNA sequences. *J. Mol. Biol. 288*, 213–229.
45. Dong, F., and Vanholde, K. E. (1991) Nucleosome positioning is determined by the (H3-H4)2 tetramer. *Proc. Natl. Acad. Sci. U.S.A. 88*, 10596–10600.
46. Davey, C. A., Sargent, D. F., Luger, K., Maeder, A. W., and Richmond, T. J. (2002) Solvent mediated interactions in the structure of the nucleosome core particle at 1.9 angstrom resolution. *J. Mol. Biol. 319*, 1097–1113.
47. Solis, F. J., Bash, R., Wang, H., Yodh, J., Lindsay, S. A., and Lohr, D. (2007) Properties of nucleosomes in acetylated mouse mammary tumor virus versus 5S arrays. *Biochemistry 46*, 5623–5634.
48. Roy, R., Kozlov, A. G., Lohman, T. M., and Ha, T. (2007) Dynamic structural rearrangements between DNA binding modes of *E. coli* SSB protein. *J. Mol. Biol. 369*, 1244.
49. Koopmans, W. J. A., Brehm, A., Logie, C., Schmidt, T., and van Noort, J. (2007) Single-pair FRET microscopy reveals mononucleosome dynamics. *J. Fluoresc. 17*, 785–795.

BI8000775